Orographic Influence on the Track Continuity Associated with the Passage of Typhoons over Central Mountain Range of Taiwan

Yuh-Lang Lin, Nicholas C. Witcraft
North Carolina State University, Raleigh, North Carolina 27511
Ying-Hwa (Bill) Kuo
National Center for Atmospheric Research
Boulder, Colorado

1. Introduction

It was found that weaker typhoons tend to be blocked by the CMR and form a secondary circulation center on the lee side making the track discontinuous, while stronger typhoons have a continuous track (e.g. Wang 1980). A brief review can be found in Chang (1982), Lin et al. (1999) and Wu and Kuo (2000) among others. Lin et al. (2004) proposed that when V_{max}/Nh is small (large), the cyclone track would be discontinuous (continuous) (Fig. 1), where V_{max} is the maximum tangential wind, N the Brunt–Väisäla frequency, and h the mountain height. In addition, a combination of small (large) V_{max}/Nh, R/L_y, U/Nh, U/fL_x, and V_{max}/fR, and large (small) h/L_x corresponds with large (small) track deflection, where R is the radius of the tropical cyclone, L_x and L_y are the E-W and N-S scales of the mountain, respectively, and U is the basic wind speed. With very strong blocking, such as very small R/L_y, the cyclone would be deflected to the south upstream of the mountain.

Lin et al. (2004) also proposed a conceptual model to explain track deflection and continuity for a westward-propagating cyclone encountering idealized Taiwan topography (Fig. 2). With weak orographic blocking, the cyclone is able to cross over the mountain range continuously with some northward deflection. With moderate orographic blocking, northward deflection upstream of the mountain range is greater and a leeside vortex forms to the southwest of the mountain range, indicative of a discontinuous cyclone track. With strong orographic blocking, the track is discontinuous and the cyclone is deflected to the south and a secondary cyclone forms to the northwest of the mountain range. The upstream northward or southward deflection is explained by the orographic blocking on the outer circulation of the cyclone.

In this study we will analyze supertyphoon Bilis (2000) and typhoon Toraji (2001). Supertyphoon Bilis hit the southeast of Taiwan with a continuous track. Typhoon Toraji was of moderate intensity and has a discontinuous track. It had a slower translation speed as it hit central Taiwan. The goal of this study is to use high-resolution numerical model to investigate the dynamics of track deflection in the vicinity of Taiwan.

2. Experiment Design

The PSU/NCAR MM5.v3 model is adopted for the numerical simulations. The NCEP 2.5°x2.5° reanalysis data is used for model initialization and for boundary conditions. The 1-km resolution terrain and land use data are used. The Bilis experiment is integrated for 48 h starting at 8/21/12Z 2000, while the Toraji experiment is run for 48 h starting at 7/28/12Z 2001. A bogus vortex of 70 ms^{-1} and 55 ms^{-1}, for Bilis and Toraji

respectively, is inserted. There are three nested domains designed for the simulations. Domains 1, 2, and 3 use 21, 7, and 2.33 km grid resolutions and have 200x200, 199x199, and 265x244 grid points in the horizontal, respectively. There are 33 stretched σ levels in vertical. The top of the model is at 50 mb. The time steps for domains 1, 2, and 3 are 30, 10, and 4 s, respectively. The Blackadar scheme is used to parameterize the PBL processes and the Goddard Lin-Farley-Orville scheme is used to parameterize the microphysical processes. For the outer domain, the Betts-Miller scheme is used to parameterize sub-grid scale convection, while no cumulus parameterization is used at 7 and 2.3 km resolution simulations.

3. Results and Discussions

3.1 Bilis

The simulated storm took a cyclonic and continuous track over the CMR, which is very similar to observations. By the time of landfall, the minimum pressure was near 930 mb, close to the observed pressure of around 920 mb from the JMA.

The lower, mid, and upper level cyclone centers remain in phase during and after passage over Taiwan. The vertical coupling of potential vorticity (PV) is excellent, with a shaft of weaker winds (the eye) extending to the tropospause. At 8/21/15Z, the center is located over the CMR. The eastern flank of PV remains vertically stacked, with the lower level PV slightly weakened by the CMR. One dramatic impact of the CMR on Bilis is the destruction of the western flank of the PV, which has lost its vertical structure. The upper-level PV has moved farther to the west, the middle level PV is weakened, and the low-level PV keeps its strength, but spreads further to the west. The asymmetry of the PV affected by the CMR at this time appears to contribute to the disappearance of the eye. A tongue of positive PV between 850 and 900 mb extending west from the CMR. This appears to be caused by the advection of warm air as the flow crosses over the CMR. If the storm were weaker and/or moving slower, as in typhoon Toraji, this tongue of positive PV would help spawn a new low-level circulation center. At 8/21/18Z, it is evident this did not occur, as the lower and upper-level PV maxima are once again vertically stacked. However, the eye is no longer an identifiable feature. The interaction with the CMR has weakened the system, with lower winds and magnitudes of PV being associated with the typhoon. For Bilis, the warming was especially intense, as can be seen from the 850 mb geopotential height and temperature fields. Downstream of the northern CMR, the air is 6-8 K warmer than on the upstream side, which appears to be caused by the advection of warm air and adiabatic warming over the lee slope. This warming has caused a distortion in the height field, with lower heights in the same area of warming. As the vortex center crossed the CMR, it took cyclonic track toward the area of warming.

Further insight can be gathered by looking at backward trajectories from the time when the vortex became well established on the west side of the CMR. Parcels at lower levels (e.g. σ=0.9) to the south of the circulation center went around the north side of the CMR, while parcels on the north side of the circulation traveled over the CMR. At σ=0.8 and 0.7, all parcels traveled over the central CMR. At σ=0.6, the southern parcels originate from

the east of Taiwan, and travel over the CMR, while the northern most parcel travels around the northern portion of the CMR, then rises up the east slope of the CMR before turning cyclonically around the circulation center.

Figure 3 shows the 850 mb geopotential height and PV during the passage of Bilis over CMR. At 8/22/14Z the cyclone center is making landfall, and the high PV near the center is easy to identify (Fig. 3a). Areas of negative PV are located on the eastern slope of the CMR, due to anticyclonic vorticity being generated against the CMR. On the western slope of the CMR, cyclonic vorticity caused by PV generation associated with blocking (e.g. Smith 1989) creates a broad area of positive PV. Flow through the mountain gaps creates alternative areas of positive and negative PV downstream. An impressive PV streamer extends from the north of Taiwan, as the air goes around the northern portion of the CMR. As the cyclone center crosses the CMR (Figs. 3b and 3c), the PV on the slopes of the CMR transitions from positive (negative) to negative (positive) on the west (east) slopes. The large PV streamer ultimately becomes wrapped up into the center once it passes over the CMR (Fig. 3d). The entrainment of this PV streamer into the circulation may help draw the center back to the south after it crosses the CMR, and is a topic of future research.

3.2 Toraji

The movement of Toraji was slower, allowing a more complicated interaction with the CMR. Unlike in Bilis, the system did not remain vertically coupled on its path over the CMR, resulting in a discontinuous track. The simulated Toraji behaved similarly to the observed Toraji. The cyclone centers remain coupled until making landfall in central Taiwan. Thereafter, a new low-level circulation center forms on the lee side of the CMR, but to the south of the extrapolated path. This secondary circulation center soon becomes the dominant center, while the old low-level center weakens and dissipates. The upper-level centers dissipate as the old primary low level centers die, and reform over the new low level center.

The vertical cross sections also portray the formation of new circulation center (not shown). At 7/29/12Z 2000, the storm has good vertical coupling, with the upper level PV maximum located over the lower level one. During the next 6 h period, the cyclone center retains its vertical coupling as it comes ashore. During the same time period, a new secondary low-level circulation center forms in the lee of the CMR. A low-level PV maximum is present to the west of the CMR, a product of advection of warm air, as well as the generation of a secondary vortex as the outer circulation of Toraji encompasses the northern CMR, due to effects of strong blocking. In addition, an area of lighter winds is present just above the low level PV, with higher winds to the west in the Taiwan Strait. By 7/29/21Z, a low-level PV maximum and circulation center has become established west of the CMR, while the upper-level PV maximum remains over the CMR. At 7/30/00Z, the new circulation center has extended in the vertical and coupled with the old upper-level PV and circulation center. Thus, for a weaker typhoon, the low-level PV is destroyed by the CMR, which gradually

weakens the mid- and upper-level PV. As the outer circulation impinges on the CMR, a new low-level PV center forms on the lee side, and ultimately takes over as the new cyclone center, and if conditions are favorable, the PV re-extends into the upper levels. The reformation process shows up even more clearly in the streamline plots.

For Toraji, the area of downslope winds shown on the 850 mb temperature field was not as extensive as for Bilis, due to the weaker winds associated with Toraji. At 7/29/17Z the typhoon is making landfall. A large area of warming is present off the northwest coast, with a smaller area in the south tip of the CMR, to the south of the center. The deformation of the geopotential height field is greater for Toraji than in Bilis. Over time, the area to the northwest becomes the focus for the formation and development of the secondary circulation center. The parcel trajectories for Toraji behaved in a different fashion from those for Bilis. At lower levels (σ = 0.9, 0.8) the parcels of Toraji tend to cross the northern portion of the CMR. At middle levels (σ = 0.7, 0.6) the parcels initially wrap into the primary vortex, then become entrained into the secondary vortex. As in Bilis, the parcels originate at low levels. Once the parcels cross the CMR, convection releases latent heat, raising the potential temperature. On the lee side of the CMR, the parcels remain at a higher level, due to their higher potential temperature.

Similar to Bilis, a banner of PV at 850 mb is present extending from the north tip of the CMR as Toraji makes landfall at 7/29/17Z (Fig. 4a). The primary difference is that the banner extends more northwesterly than for Bilis. The PV banner is also located closer to the area of greatest warming. By 7/29/21Z (Fig. 4c), the PV banner has wrapped into the secondary vortex center, and by 7/29/23Z (Fig. 4d) it has become the primary vortex center. The combination of warming and the vorticity banner appear to have generated a PV maximum on the lee side of the northern CMR, helping to generate the secondary center, which ultimately became dominant.

3.3 Control parameters for Bilis and Toraji

Based on the control experiments, the nondimensional control parameters proposed in Lin et al. (2004) are estimated as ($V_{\max}/Nh$, U/Nh , R/L_y) = (2.0, .27, .26) and (1.67, .20, .22) for Bilis and Toraji, respectively. The corresponding dimensional parameters are: (a) $V_{\max} = 60\ ms^{-1}$, $U = 8\ ms^{-1}$, $h = 3000\ m$, $N = 0.01 s^{-1}$, $R = 60\ km$, and $L_y = 230\ km$ for Bilis; and (b) $V_{\max} = 50\ ms^{-1}$, $U = 5.9\ ms^{-1}$, $h = 3000\ m$, $N = 0.01 s^{-1}$, $R = 50\ km$, and $L_y = 230\ km$ for Toraji. These flow parameters are estimated when the typhoons moved close to Taiwan, but before they made the landfall. The third control parameter, R/L_y, is estimated from satellite and radar imagery. Compared with the regime diagram as shown in Fig. 1, both Bilis and Toraji belonged to the regime of continuous track. For Bilis this is consistent with observations and numerical modeling results, while for Toraji the observed and simulated track was discontinuous. However, Toraji was near the regime boundary zone ($1.2 < V_{\max}/Nh < 1.6$) for a discontinuous vs.

discontinuous track. As seen in the low-level streamline analysis, the remnants of the low-level survived the transit over the CMR to become entrained into the secondary center.

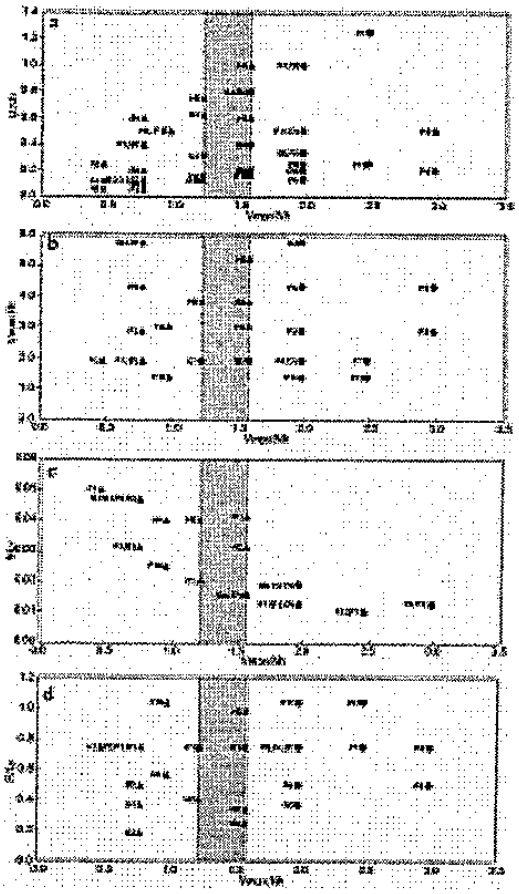

Fig. 1: Continuous (filled circles) and discontinuous (triangles) tracks in the parameter spaces of: (a) U/Nh, (b) V_{max}/Rf, (c) h/L_x, and (d) R/L_y vs. V_{max}/Nh, based on idealized simulations. The track is continuous (discontinuous) to the right (left) of the shaded zones. (From Lin et al. 2004)

Acknowledgments Discussions with Dr. Simon Chang at NRL is appreciated. This research is supported by UCAR Coop. Agreement under NSF ATM-9732665 and ONR N00014-02-1-0674.

References Upon request

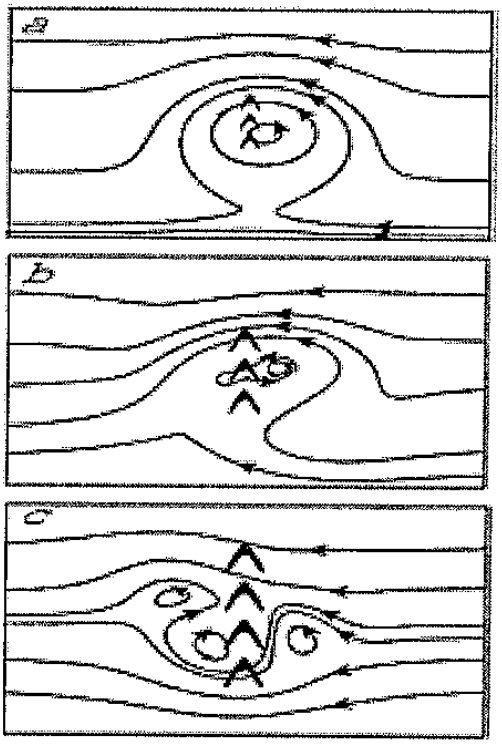

Fig. 2: A conceptual model for track deflection for a westward propagating cyclone to orographic blocking: (a) weak blocking, (b) moderate blocking, and (c) strong blocking. See text for details. (From Lin et al. 2004)

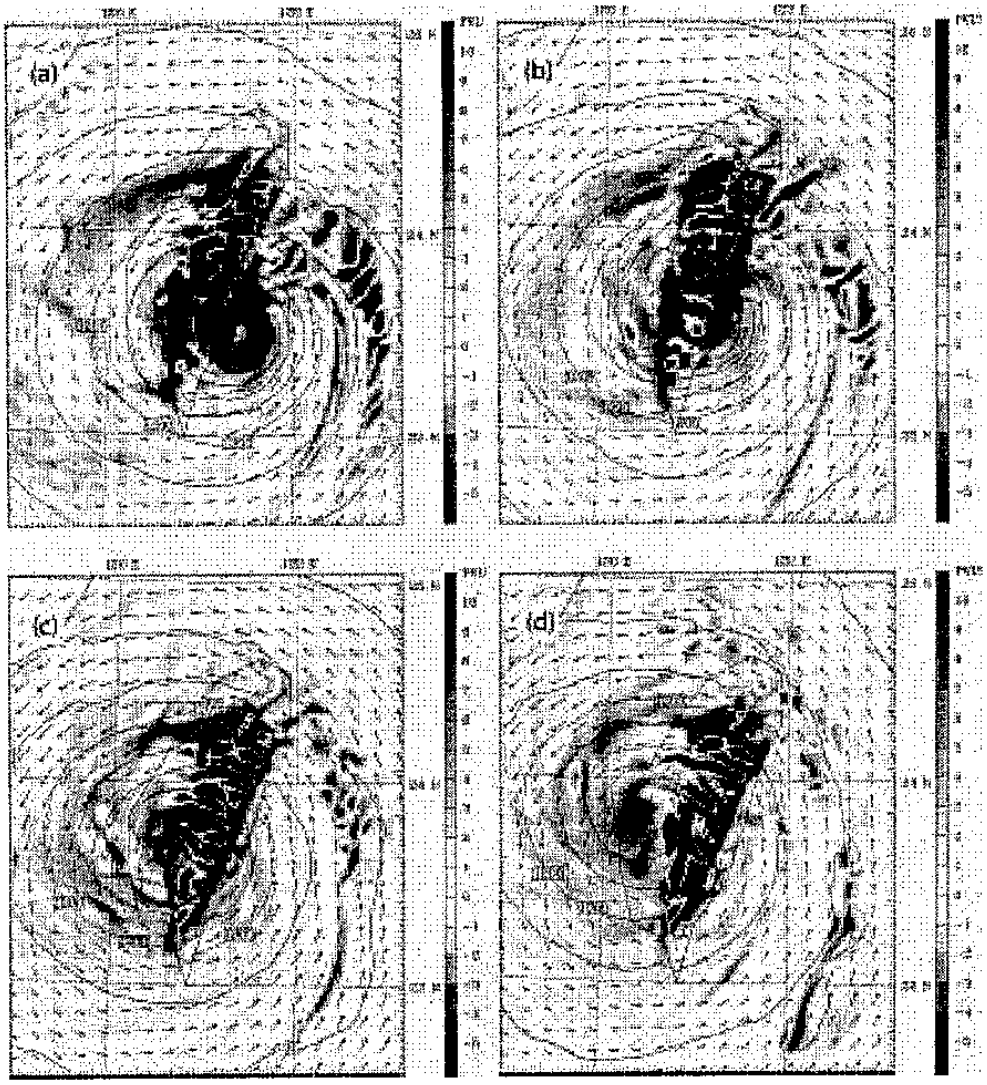

Fig. 3: The 850 mb geopotential height, PV, and wind vectors for Supertyphoon Bilis at (a) 8/22/14Z, (b) 8/22/15Z, (c) 8/22/16Z, and (d) 8/22/17Z 2000.

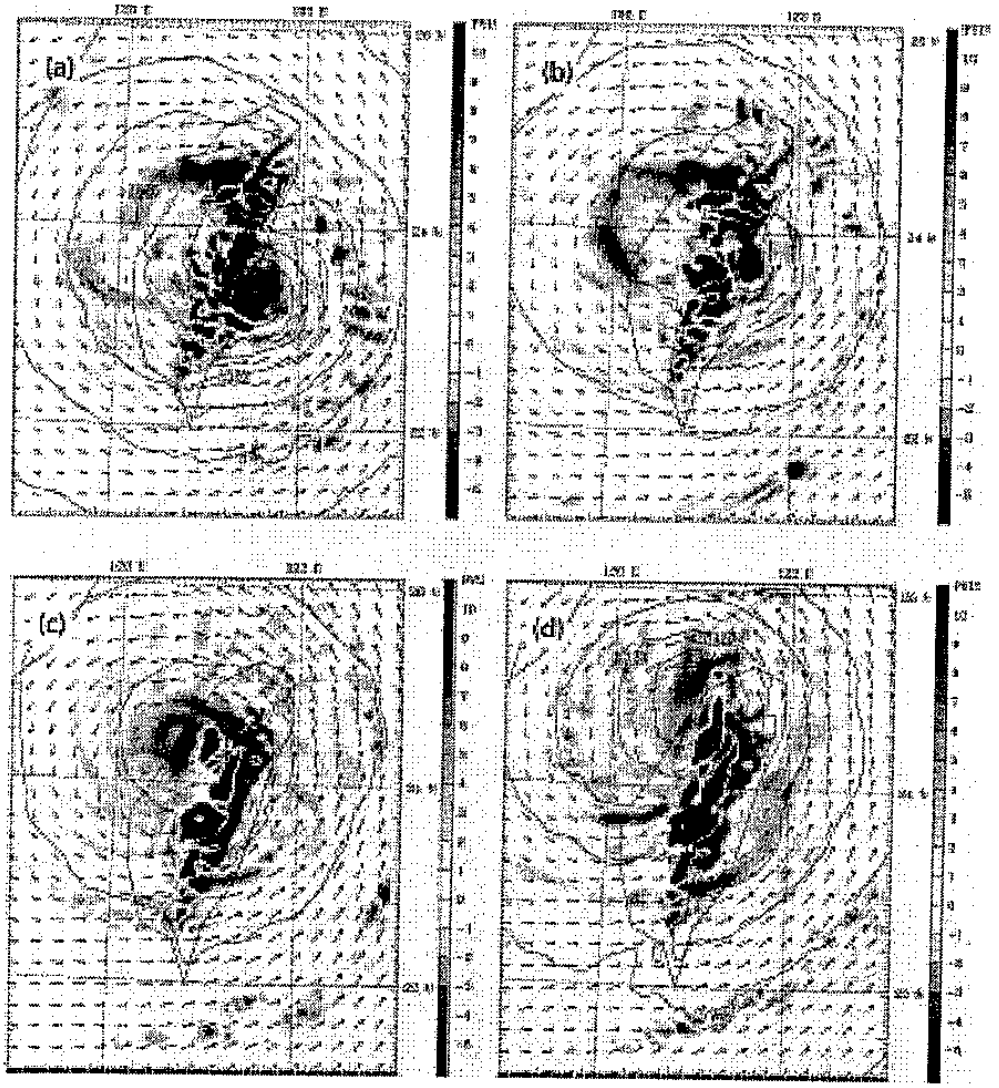

Fig. 4: The 850 mb geopotential height, PV, and wind vectors for Typhoon Toraji at (a) 7/29/17Z, (b) 7/29/19Z, (c) 7/29/21Z, and (d) 7/29/23Z July 2001.